

**UCLA**  
**COMPUTATIONAL AND APPLIED MATHEMATICS**

---

**Two-Grid Method for Linear Elasticity on  
Unstructured Meshes**

**Petr Vanek  
Marian Brezina  
Radek Tezaur**

**August 1999  
CAM Report 99-28**

---

**Department of Mathematics  
University of California, Los Angeles  
Los Angeles, CA. 90095-1555**

**<http://www.math.ucla.edu/applied/cam/index.html>**

## TWO-GRID METHOD FOR LINEAR ELASTICITY ON UNSTRUCTURED MESHES\*

PETR VANĚK<sup>†</sup>, MARIAN BREZINA<sup>‡</sup>, AND RADEK TEZAU<sup>†</sup>

**Abstract.** We propose an abstract two-grid algorithm with convergence independent of the coarse-space size. The abstract algorithm is applied to problems of three-dimensional linear elasticity discretized on unstructured meshes. With no regularity assumptions we prove uniform convergence with respect to coarse-space size, domain, essential boundary conditions, and jumps in Young modulus. Numerical experiments confirm the theory and show that the method works well even if some assumptions of the theory are violated.

**Key words.** Convergence independent of the coarse space size, unstructured meshes, black-box solver, smoothed tentative prolongator, three-dimensional elasticity.

**AMS subject classifications.** 65F10, 65N55

**1. Introduction.** The standard multigrid formulation of the two-level method suffers from the dependence of the rate of convergence on the size of the coarse space. When solving an elliptic problem of order  $2k$ , assuming no regularity, the rate of convergence can be estimated by  $1 - C(\frac{h}{H})^{2k}$ . Here  $H$  and  $h$  denote the characteristic meshsizes on the coarse and fine levels, respectively. This estimate poses a strict limitation on the size of the coarse space if good convergence is to be guaranteed. Similar obstacles are also encountered when other techniques are used (e.g., [11]).

Today's two-level domain decomposition preconditioners typically offer an improvement by yielding condition numbers bounded polylogarithmically in  $\frac{H}{h}$  (e.g., [5, 13, 17]). The direct local solvers used by these methods, however, result in large computational complexity, while application of inexpensive approximate subdomain solvers may not guarantee the optimal condition number estimate [3, 6, 10].

We suggest a method with coarse-space size independent convergence diminishing significantly these difficulties. Our algorithm is based on a concept of smoothed tentative prolongator introduced in [19] and further investigated in [16, 22]. Our tentative coarse space is derived from a system of nonoverlapping subdomains and supports rigid body modes in a local sense. Coarse-space basis has very small overlaps of supports; the columns of the tentative prolongator associated with two different subdomains have disjoint nonzero structure. A special polynomial smoother is applied to the tentative prolongator, which extends the supports but only so much that their intersections remain bounded. Our choice of the prolongator smoother, pre-smoother and post-smoother enables us to prove convergence independent of the coarse-space size. The price we have to pay for having a coarse space of modest size, in terms of computational complexity, is much smaller in our case than it is for standard domain decomposition methods with direct subdomain solvers. Denoting the average number of nodes per three-dimensional (3D) subdomain by  $N_d$ , the recommended degree of the prolongator smoother is  $\lfloor \frac{1}{2}(N_d^{1/3} - 1) \rfloor$ . Consequently, the asymptotic computational

---

\*This research was supported by NSF grants ASC-9121431, ASC-9217394, and ASC-9404734 and the Czech academic grant VS 97156.

<sup>†</sup>Center for Computational Mathematics, University of Colorado at Denver, Denver, CO 80217-3364 (pvanek@math.cudenver.edu, rtezaur@math.cudenver.edu).

<sup>‡</sup>Department of Applied Mathematics, University of Colorado at Boulder, Boulder CO 80309-0526 (brezina@newton.colorado.edu).

cost associated with treating one subdomain is  $O(N_d^{4/3})$ . This contrasts with  $O(N_d^{7/3})$  operations needed during the factorization of the local problem when using direct subdomain solvers. Based on our experience, internal iterative solvers tend to have a negative impact on the robustness of the method. On the theoretical front, it is the belief of the authors that in order to carry out good convergence estimates for the iterative coarse-level solver, one has to impose additional assumptions. This is most pronounced when solving problems with coefficient jumps. For the above reasons, we decided to use the direct coarse-level problem solver. We show that the computational cost is quite low even if a naïve (Cholesky) coarse-level solver is used. For the coarse space of optimal size the overall computational complexity of our method applied to the problems of 3D elasticity is  $O(n^{7/6})$  and  $O(n^{6/5})$  in the planar case.

The theory presented in this paper is based on the unpublished technical report [20]. An extended abstract of this paper, dealing with the simpler case of scalar elliptic equations, has been published in [24]. A simplified theory and construction of the coarse spaces, unobscured by issues specific to elasticity, may be found there.

We find it convenient to divide the analysis into two parts: an abstract theory that yields a coarse-space size independent convergence, provided that our assumptions on the components of the method are satisfied, and verification of the assumptions for the case of 3D elasticity.

Based on our experience with industrial models, it is desirable to design methods with convergence properties independent of boundary conditions. In designing robust methods for solving elasticity problems, one must not rely solely on the coercivity of the bilinear form guaranteed by the boundary conditions. The reason for this is that the constant in Korn's inequality is often very small. Moreover, arguments using the "global" coercivity are usually difficult to use in the case of nonscalar equations with jumps in coefficients. For these reasons, we employ a coarse space supporting local kernels of the bilinear form. The analysis of this coarse space can be carried out using local arguments on the factorspace modulo rigid body modes, and the assumptions on the essential boundary conditions are no longer needed. This contrasts with earlier works (e.g., [2]), whose analysis relies on essential boundary conditions. Furthermore, based on empirical observations, we suggest to solve the problem with a matrix obtained by block-diagonal scaling of the original stiffness matrix. This requirement is not essential to the analysis and slightly complicates the theory, but it is of considerable computational value. Qualitatively the same result can be obtained assuming only diagonal scaling, but we deem the scaling by block diagonal more natural for treating nonscalar equations.

For problems with large jumps in Young modulus, our theory requires each subdomain to be a union of a bounded number of star-shaped domains with large overlaps. This is more restrictive than the shape-regularity requirement formulated using a locally Lipschitz one-to-one mapping in the scalar case. However, in the case of uniformly bounded coefficients such an assumption is not necessary.

The paper is organized as follows. The abstract algorithm and analysis are presented in section 2. Section 3 deals with the construction of the tentative coarse space suitable for real-life problems of solids discretized on unstructured meshes. Requirements on the system of subdomains for our construction of the tentative prolongator as well as theoretical tools needed for the application of the abstract theory are the subject of section 4. Section 5 presents the convergence result independent of the coarse-space size, domain, essential boundary conditions, and jumps in Young modulus provided the subdomains are aligned with the jumps. The

estimate of computational complexity  $O(n^{7/6})$  for the optimal size coarse space is also given here. Finally, numerical experiments of section 6 confirm the theoretical results and show robustness of the method even if applied to problems not in the scope of the current theory.

**2. Abstract framework.** In this section we develop and analyze a simple two-grid abstract method for the numerical solution of a system of linear algebraic equations

$$(1) \quad \mathbf{Ax} = \mathbf{b}$$

with a symmetric positive definite  $n \times n$  matrix  $A$ . The method is determined by two components: a *tentative prolongator*  $P : \mathbb{R}^m \rightarrow \mathbb{R}^n$  ( $m \ll n$ ) and a symmetric *prolongator smoother*  $M \in [\mathbb{R}^n]$  that commutes with  $A$ . The proposed method is, up to a post-processing step, the standard variational two-level scheme with a smoothed prolongator  $MP$  and special smoothing procedures derived from  $M$ . The construction of such smoothers is motivated by an attempt to reduce the error components which cannot be represented in the coarse space.

Let us set

$$(2) \quad A_M = M^2 A, \quad M' = I - \frac{\omega}{\bar{\varrho}(A_M)} A_M,$$

where  $\omega \in (0, 2)$  is a given parameter and  $\bar{\varrho}(A_M)$  is a known upper bound of the spectral radius  $\varrho(A_M)$ . We define the presmoothers  $\mathbf{x} \leftarrow \mathcal{S}_M(\mathbf{x}, \mathbf{b})$  and the postsmoothers  $\mathbf{x} \leftarrow \mathcal{S}_{M'}(\mathbf{x}, \mathbf{b})$  to be linear iterative methods consistent with (1) such that their error propagation operators are matrices  $M$  and  $M'$ , respectively. Note that such methods can be easily constructed if  $M$  is a polynomial in  $A$ . The algorithm can be written down as follows.

**ALGORITHM 2.1.** For the given initial guess  $\mathbf{x} \in \mathbb{R}^n$ ,

repeat

1.  $\mathbf{x} \leftarrow \mathcal{S}_M(\mathbf{x}, \mathbf{b})$ ,
2. solve  $P^T M A M P \mathbf{v} = P^T M (\mathbf{Ax} - \mathbf{b})$ ,
3.  $\mathbf{x} \leftarrow \mathbf{x} - M P \mathbf{v}$ ,
4.  $\mathbf{x} \leftarrow \mathcal{S}_{M'}(\mathbf{x}, \mathbf{b})$

until convergence;

5. Post process  $\mathbf{x} \leftarrow \mathcal{S}_M(\mathbf{x}, \mathbf{b})$ .

*Remark 2.2.* Steps 1–4 of the algorithm above form the standard two-level multigrid method given by prolongator  $MP$  and smoothers  $\mathcal{S}_M, \mathcal{S}_{M'}$ . For such an algorithm, the theory presented here gives the error estimate in the  $A_M$ -seminorm. The practical value of this estimate is undermined by the fact that  $A_M$  depends on the coarse space, as using a smaller coarse space requires a more powerful smoother  $M$  to get the optimal convergence result.

The post-processing allows us to prove the  $A$ -norm error estimate in the form

$$\|\mathbf{e}_i^M\|_A^2 \leq (1 - C)^i \|\mathbf{e}_0\|_A^2,$$

where  $\mathbf{e}_i^M$  is the error  $\mathbf{e}_i$  post-processed by step 5. As  $M$  is the presmoothers and the remaining parts of the algorithm do not enlarge the  $A$ -norm of the error, without step 5 we could still prove

$$\|\mathbf{e}_i\|_A^2 \leq (1 - C)^{i-1} \|\mathbf{e}_0\|_A^2,$$

a somewhat weaker estimate.  $\square$

Throughout the paper, we use  $\langle \cdot, \cdot \rangle$  and  $\|\cdot\|$  to denote the Euclidean scalar product and the associated norm. For a symmetric positive (semi)definite matrix  $B$ , we define  $B$ -(semi)norm  $\|\cdot\|_B = \langle B\cdot, \cdot \rangle^{1/2}$ . Symbols  $\perp$ ,  $\perp_B$  will denote the orthogonal complement with respect to the Euclidean and  $B$ -scalar products, respectively. Symbol  $Z|_S$  will be used for the restriction of a mapping  $Z$  to a subspace  $S$ .

The following assumption specifies requirements on  $M$ ,  $P$ , and  $\bar{\varrho}(A_M)$  needed for proving the coarse-space size independent convergence.

**ASSUMPTION 2.3.** *There exists a constant  $C_1 > 0$  independent of  $m$ ,  $n$  such that*

1. *There is a linear mapping  $Q_C : \mathbb{R}^n \rightarrow \text{Range}(P)$  that satisfies*

$$(3) \quad \|(I - Q_C)\mathbf{u}\| \leq \frac{C_1}{\sqrt{\bar{\varrho}(A_M)}} \|\mathbf{u}\|_A \quad \forall \mathbf{u} \in \mathbb{R}^n,$$

where  $\bar{\varrho}(A_M)$  is an upper bound of  $\varrho(A_M)$  used in (2);

2. *the prolongator smoother  $M$  is symmetric, commutes with  $A$ , and satisfies  $\varrho(M) \leq 1$ .*

A suitable choice of the prolongator smoother  $M$  and of the corresponding estimate  $\bar{\varrho}(A_M)$  will be given in Algorithm 2.7 and Lemma 2.8.

*Remark 2.4.* In comparison, both the standard two-level theory [8] and the regularity-free multilevel theory introduced in [7] (see also [4]), applied to the case of two levels, use the assumption that

$$(4) \quad \|(I - Q_C)\mathbf{u}\| \leq \frac{C'}{\sqrt{\varrho(A)}} \|\mathbf{u}\|_A \quad \forall \mathbf{u} \in \mathbb{R}^n$$

and give a convergence rate estimate which depends on  $C'$ .

If  $\bar{\varrho}(A_M) \ll \varrho(A)$ , condition (3) is significantly weaker than (4). At the end of this section we will construct  $M$  as a polynomial in  $A$  such that  $\varrho(A_M) \leq C \deg(M)^{-2} \varrho(A)$ . For verification of Assumption 2.3 for a simple model case, see Example 2.12.  $\square$

Let us recall that  $\omega$  is the damping parameter from the definition (2) of  $M'$ . The following theorem provides an abstract convergence estimate.

**THEOREM 2.5.** *Let  $\mathbf{e}_i$  denote the error after  $i$  iterations given by steps 1–4 of Algorithm 2.1, and let  $\mathbf{e}_i^M = M\mathbf{e}_i$  be the error  $\mathbf{e}_i$  smoothed by step 5. Then, under Assumption 2.3, it holds that*

$$(5) \quad \|\mathbf{e}_{i+1}\|_{A_M}^2 \leq (1 - C_2) \|\mathbf{e}_i\|_{A_M}^2$$

and

$$(6) \quad \|\mathbf{e}_i^M\|_A^2 \leq (1 - C_2)^i \|\mathbf{e}_0\|_A^2,$$

where

$$(7) \quad C_2(\omega) = \frac{\omega(2 - \omega)}{C_1^2 + \omega(2 - \omega)} \leq C_2(1) = \frac{1}{C_1^2 + 1}, \quad \omega \in (0, 2).$$

*Remark 2.6.* The following considerations allow us to disregard the fact that  $M$  may be a singular matrix in the proof of Theorem 2.5. The reader who is not interested in technical details may assume that  $M$  is invertible and proceed directly to the proof.

The error propagation operator corresponding to steps 1–4 of Algorithm 2.1 is given by

$$(8) \quad E = M' (I - MP(P^T A_M P)^+ P^T MA) M,$$

where  $+$  denotes a pseudoinverse. Since  $\text{Ker}(P^T A_M P) = \{\mathbf{x} \in \mathbb{R}^m : P\mathbf{x} \in \text{Ker}(M)\}$ , the algorithm is independent of a particular choice of the pseudoinverse.

From (8),  $\text{Ker}(M) \subset \text{Ker}(E)$ , and it is sufficient to investigate the error propagation operator  $E$  on the space  $V \equiv \text{Ker}(M)^\perp$ . From (2) and from the assumption that  $A, M$  commute, it follows that  $A, M, A_M, M'$  commute mutually. Therefore their eigenvectors coincide and  $V$  is their common invariant subspace. Therefore, the matrices  $A, M, M'$ , and  $A_M$  can be understood as linear mappings from  $V$  onto  $V$ , and  $M$  and  $A_M$  are invertible on  $V$ . We redefine the tentative prolongator  $P$  as  $P \leftarrow Q_M P$ , where  $Q_M$  is the projector onto  $V$  orthogonal with respect to Euclidean inner product. By redefining the components, we did not change the error propagation operator  $E$  on  $V$ . Also, Assumption 2.3 remains valid for all vectors  $\mathbf{u} \in V$  and the redefined tentative prolongator  $P$ .

Throughout the proof, any fine-level vector is a vector from  $V$ , and an orthogonal complement is understood as an orthogonal complement in  $V$ . This view will allow us to carry out the proof formally the same as if  $M$  were always nonsingular.  $\square$

*Proof.* In view of Remark 2.6, we can assume that  $M$  is invertible.

By direct computation, the error propagation operator  $E : \mathbf{e}_i \mapsto \mathbf{e}_{i+1}$  from (8) can be rewritten as

$$(9) \quad E = M' M (I - P(P^T A_M P)^+ P^T A_M).$$

From the definition of  $A_M, \mathbf{e}_i^M$ , and the fact that  $M$  is symmetric and commutes with  $A$ , we have

$$\begin{aligned} \|\mathbf{e}_i^M\|_A &= \|\mathbf{e}_i\|_{A_M}, \\ \|\mathbf{e}_0\|_{A_M} &\leq \varrho(M) \|\mathbf{e}_0\|_A \leq \|\mathbf{e}_0\|_A, \end{aligned}$$

as  $\varrho(M) \leq 1$  is assumed. Therefore, the  $A$ -norm estimate (6) follows from (5). In the rest of the proof we estimate the error propagation operator  $E$  in the  $A_M$ -norm.

*Step 1.* The coarse-level correction part  $R$  of the error propagation operator  $E$  from (9),

$$R = I - P(P^T A_M P)^+ P^T A_M$$

is the  $A_M$ -orthogonal projection onto  $\text{Range}(P)^\perp_{A_M}$ . It is routine to verify that

$$(10) \quad T \equiv \text{Ker}(P^T A_M) = \text{Range}(P)^\perp_{A_M},$$

so  $T = \text{Range}(R)$ , and

$$(11) \quad \|E\|_{A_M} = \|M' M R\|_{A_M} \leq \|(M' M)|_T\|_{A_M} \|R\|_{A_M} = \max_{\mathbf{x} \in T \setminus \{0\}} \frac{\|M' M \mathbf{x}\|_{A_M}}{\|\mathbf{x}\|_{A_M}}.$$

From (2) and the assumption that  $A, M$  are symmetric matrices that commute, it follows that matrices  $A, M, M', A_M$  commute mutually and are both symmetric and  $A_M$ -symmetric. Hence, for every fine-level vector  $\mathbf{x}$ ,

$$\begin{aligned} \|M' M \mathbf{x}\|_{A_M} &\leq \varrho(M') \|M \mathbf{x}\|_{A_M} \leq \|M \mathbf{x}\|_{A_M}, \\ \|M M' \mathbf{x}\|_{A_M} &\leq \varrho(M) \|M' \mathbf{x}\|_{A_M} \leq \|M' \mathbf{x}\|_{A_M}, \end{aligned}$$

as  $\varrho(M) \leq 1$  and  $\varrho(M') \leq 1$ . Thus, (11) can be rewritten as

$$(12) \quad \|E\|_{A_M} \leq \max_{\mathbf{x} \in T \setminus \{0\}} \frac{\|M'M\mathbf{x}\|_{A_M}}{\|\mathbf{x}\|_{A_M}} \leq \max_{\substack{\mathbf{x} \in T \\ \mathbf{x} \neq 0}} \min \left\{ \frac{\|M\mathbf{x}\|_{A_M}}{\|\mathbf{x}\|_{A_M}}, \frac{\|M'\mathbf{x}\|_{A_M}}{\|\mathbf{x}\|_{A_M}} \right\}.$$

Inequality (12) allows the following interpretation: For any fixed  $\mathbf{x} \in \text{Range}(R) \setminus \{0\}$ , the effect of the product of smoothers,  $\|M'M\mathbf{x}\|_{A_M}/\|\mathbf{x}\|_{A_M}$ , can be estimated in terms of the effect of the more efficient of the two smoothers  $M, M'$ .

In the rest of the proof, we will show that for any  $\mathbf{x} \in T \setminus \{0\}$ , at least one of the expressions in the minimum above is bounded by  $1 - C_2$ , where  $C_2$  is given in (7).

*Step 2.* In this step we show that for any fixed  $\mathbf{x} \in T \setminus \{0\}$ , the effect of the smoother  $M'$  increases with decreasing effect (i.e.,  $\frac{\|M\mathbf{x}\|_{A_M}}{\|\mathbf{x}\|_{A_M}} \rightarrow 1$ ) of the smoother  $M$ . More precisely, we show that

$$(13) \quad \frac{\|M'\mathbf{x}\|_{A_M}^2}{\|\mathbf{x}\|_{A_M}^2} \leq 1 - \frac{\|M\mathbf{x}\|_{A_M}^2}{\|\mathbf{x}\|_{A_M}^2} \frac{\omega(2-\omega)}{C_1^2} \quad \forall \mathbf{x} \in T \setminus \{0\}.$$

To this end, we first estimate for any fine-level vector  $\mathbf{x} \neq 0$ :

$$\begin{aligned} \|M'\mathbf{x}\|_{A_M}^2 &= \left\| \left( I - \frac{\omega}{\bar{\varrho}(A_M)} A_M \right) \mathbf{x} \right\|_{A_M}^2 \\ &= \|\mathbf{x}\|_{A_M}^2 - 2 \frac{\omega}{\bar{\varrho}(A_M)} \|A_M \mathbf{x}\|^2 + \left( \frac{\omega}{\bar{\varrho}(A_M)} \right)^2 \|A_M \mathbf{x}\|_{A_M}^2 \\ &\leq \|\mathbf{x}\|_{A_M}^2 - 2 \frac{\omega}{\bar{\varrho}(A_M)} \|A_M \mathbf{x}\|^2 + \frac{\omega^2}{\bar{\varrho}(A_M)} \|A_M \mathbf{x}\|^2 \\ &= \|\mathbf{x}\|_{A_M}^2 \left( 1 - \frac{\omega(2-\omega)}{\bar{\varrho}(A_M)} \frac{\|A_M \mathbf{x}\|^2}{\|\mathbf{x}\|_{A_M}^2} \right), \end{aligned}$$

that is,

$$(14) \quad \frac{\|M'\mathbf{x}\|_{A_M}^2}{\|\mathbf{x}\|_{A_M}^2} \leq 1 - \frac{\omega(2-\omega)}{\bar{\varrho}(A_M)} \frac{\|A_M \mathbf{x}\|^2}{\|\mathbf{x}\|_{A_M}^2}.$$

From  $AM = MA$  and the definition of  $A_M$ , it follows that  $\|M^2\mathbf{x}\|_A = \|M\mathbf{x}\|_{A_M}$ . Hence,

$$(15) \quad \frac{\|A_M \mathbf{x}\|}{\|\mathbf{x}\|_{A_M}} = \frac{\|A_M \mathbf{x}\|}{\|M^2\mathbf{x}\|_A} \frac{\|M^2\mathbf{x}\|_A}{\|\mathbf{x}\|_{A_M}} = \frac{\|AM^2\mathbf{x}\|}{\|M^2\mathbf{x}\|_A} \frac{\|M\mathbf{x}\|_{A_M}}{\|\mathbf{x}\|_{A_M}}.$$

Now, consider  $\mathbf{x} \in T \setminus \{0\}$ , and set  $\mathbf{u} = M^2\mathbf{x}$ . As  $AM = MA$ , (10) gives  $T = \text{Ker}(P^T AM^2)$  and

$$(16) \quad \mathbf{u} \in \text{Ker}(P^T A) = \text{Range}(P)^{\perp A}.$$

We estimate the ratio  $\|AM^2\mathbf{x}\|/\|M^2\mathbf{x}\|_A$  in (15) using the standard orthogonality argument: The mapping  $Q_C$  satisfying the weak approximation condition (3) returns a vector in  $\text{Range}(P)$ ; hence (16) implies  $\langle \mathbf{u}, Q_C \mathbf{u} \rangle = 0$ , and

$$\begin{aligned} \|\mathbf{u}\|_A^2 &= \langle A\mathbf{u}, \mathbf{u} \rangle = \langle A\mathbf{u}, \mathbf{u} - Q_C \mathbf{u} \rangle \leq \|A\mathbf{u}\| \|\mathbf{u} - Q_C \mathbf{u}\| \\ &\leq C_1 \bar{\varrho}(A_M)^{-1/2} \|A\mathbf{u}\| \|\mathbf{u}\|_A. \end{aligned}$$

This estimate and  $\mathbf{u} = M^2 \mathbf{x}$  yield

$$\frac{\|AM^2 \mathbf{x}\|}{\|M^2 \mathbf{x}\|_A} = \frac{\|A\mathbf{u}\|}{\|\mathbf{u}\|_A} \geq \frac{\sqrt{\hat{\varrho}(A_M)}}{C_1}.$$

Substituting the last estimate into (15), we get

$$\frac{\|A_M \mathbf{x}\|^2}{\|\mathbf{x}\|_{A_M}^2} \geq \frac{\hat{\varrho}(A_M)}{C_1^2} \frac{\|M \mathbf{x}\|_{A_M}^2}{\|\mathbf{x}\|_{A_M}^2} \quad \forall \mathbf{x} \in T \setminus \{0\}.$$

This, together with (14), completes the proof of (13).

*Step 3.* As  $\varrho(M) \leq 1$  and  $M$  is both symmetric and  $A_M$ -symmetric,  $\|M \mathbf{x}\|_{A_M} / \|\mathbf{x}\|_{A_M} \in [0, 1]$  for every nonzero fine-level vector  $\mathbf{x}$ . Thus, (12) and (13) give

$$\begin{aligned} \|E\|_{A_M}^2 &\leq \max_{\substack{\mathbf{x} \in T \\ \mathbf{x} \neq 0}} \min \left\{ \frac{\|M \mathbf{x}\|_{A_M}^2}{\|\mathbf{x}\|_{A_M}^2}, \frac{\|M' \mathbf{x}\|_{A_M}^2}{\|\mathbf{x}\|_{A_M}^2} \right\} \\ &\leq \max_{\substack{\mathbf{x} \in T \\ \mathbf{x} \neq 0}} \min \left\{ \alpha(\mathbf{x}), 1 - \alpha(\mathbf{x}) \frac{\omega(2 - \omega)}{C_1^2} \right\}, \quad \text{where } \alpha(\mathbf{x}) = \frac{\|M \mathbf{x}\|_{A_M}^2}{\|\mathbf{x}\|_{A_M}^2} \\ &\leq \max_{\alpha \in [0, 1]} \min \left\{ \alpha, 1 - \alpha \frac{\omega(2 - \omega)}{C_1^2} \right\}. \end{aligned}$$

This expression is bounded by  $(1 + C_1^{-2} \omega(2 - \omega))^{-1}$ , completing the proof.  $\square$

In the rest of this section we construct the prolongator smoother  $M$ . To do so, we need an upper bound  $\hat{\varrho}$  such that

$$(17) \quad \varrho(A) \leq \hat{\varrho} \leq C_\varrho \varrho(A).$$

The ‘‘quality’’ of the prolongator smoother depends on the magnitude of constant  $C_\varrho$ .

**ALGORITHM 2.7.** *For the given matrix  $A$ , its spectral radius estimate  $\hat{\varrho}$ , and the desired degree  $d_M$ , create the prolongator smoother  $M$  as follows:*

1. *Initialize*

$$(18) \quad \hat{\varrho}_i = \frac{\hat{\varrho}}{9^i} \quad \text{for } i = 0, 1, \dots$$

2. *Set  $M = M_K$ , where*

$$(19) \quad M_K = \left( I - \frac{4}{3} \hat{\varrho}_0^{-1} A_0 \right) \left( I - \frac{4}{3} \hat{\varrho}_1^{-1} A_1 \right) \dots \left( I - \frac{4}{3} \hat{\varrho}_{K-1}^{-1} A_{K-1} \right),$$

*matrices  $A_i$  are defined recurrently by*

$$(20) \quad A_i = \left( I - \frac{4}{3} \hat{\varrho}_{i-1}^{-1} A_{i-1} \right)^2 A_{i-1} \quad \text{for } i > 0, \quad A_0 = A,$$

*and  $K$  is chosen so that the degree  $\deg(M_K)$  is closest to the desired value  $d_M$ .*



It is easy to see that for  $M_K$  in (19) it holds that

$$(21) \quad \deg(M_K) = \frac{3^K - 1}{2}.$$

Therefore, Algorithm 2.7 can create polynomials of degrees 1, 4, 13, etc. An alternative construction capable of generating suitable polynomial of any degree has recently been given in [23].

The following lemma gives an estimate  $\bar{\varrho}(A_M) \geq \varrho(A_M)$  needed in (2).

LEMMA 2.8. *Let the prolongator smoother  $M$  be defined by Algorithm 2.7. Then*

$$(22) \quad \varrho(A_M) \leq \bar{\varrho}(A_M) = \frac{C_\varrho}{(2\deg(M) + 1)^2} \varrho(A) \leq \frac{C_\varrho}{4} \deg(M)^{-2} \varrho(A),$$

where  $C_\varrho$  is the constant from (17).

*Proof.* First, by induction we prove  $\varrho(A_i) \leq \hat{\varrho}_i$ , with  $\hat{\varrho}_i$  defined in (18). For  $i = 0$ , the inequality holds by (17). Assume it holds for  $j \leq i$ ; then, by (20) and the inductive assumption,

$$\varrho(A_{i+1}) = \max_{t \in \sigma(A_i)} \left(1 - \frac{4}{3} \hat{\varrho}_i^{-1} t\right)^2 t \leq \max_{t \in [0, \hat{\varrho}_i]} \left(1 - \frac{4}{3} \hat{\varrho}_i^{-1} t\right)^2 t \leq \frac{1}{9} \hat{\varrho}_i = \hat{\varrho}_{i+1}.$$

Hence,  $\varrho(A_K) \leq 9^{-K} \hat{\varrho}$ . Now, from (20), we find  $A_M = M^2 A = A_K$ . Finally, we obtain (22) by simple manipulations from (17) and (21).  $\square$

*Remark 2.9.* Although the method being proposed utilizes only two grids, there is a certain relationship between this method and the standard  $V$ -cycle which deserves an explanation. Note that  $M_K$  in Algorithm 2.7 is a product of about  $\log_3(n/m)$  smoothers of the form  $I - \frac{4}{3} \hat{\varrho}_k^{-1} A_k$ . This is roughly the number of levels we would obtain if we chose to use classic  $V$ -cycle multigrid with coarsening by a factor of 3 in each direction before reaching the coarse space of dimension  $m$ . Intuitively, the smoother  $I - \frac{4}{3} \hat{\varrho}_k^{-1} A_k$  in (19) plays the same role here as the smoother on level  $k$  in  $V$ -cycle, which is the similarity between our two-level method and the multigrid  $V$ -cycle.

The essential difference between the two methods is that our method applies all the smoothers on the fine level, which results in some additional computational cost. The advantage of this approach is the ability to prove uniform convergence with respect to the coarse-space size and a large class of parameters of the problem. This can be done without using full elliptic regularity or any of the nontrivial stronger approximation properties which require using tools relying heavily on the geometry of the mesh.  $\square$

*Remark 2.10.* If the prolongator smoother  $M$  is defined by Algorithm 2.7, where the choice  $M = M_K$  in Step 2 is replaced by  $M = M_{K+1}$ , we obtain acceleration in the following sense. Assuming  $\omega = 1$  in (2), in order to achieve the error reduction of one step of the method with  $M = M_{K+1}$ , one has to perform on the average at least  $\alpha_M$  steps of the method with  $M = M_K$ , where

$$\alpha_M = \frac{\log(1 - \frac{9}{C_1^2 + 9})}{\log(1 - \frac{1}{C_1^2 + 1})}.$$

This expression is an increasing function of  $C_1$  with

$$\lim_{C_1 \rightarrow \infty} \alpha_M(C_1) = 9, \quad \lim_{C_1 \rightarrow 0+} \alpha_M(C_1) = 1.$$

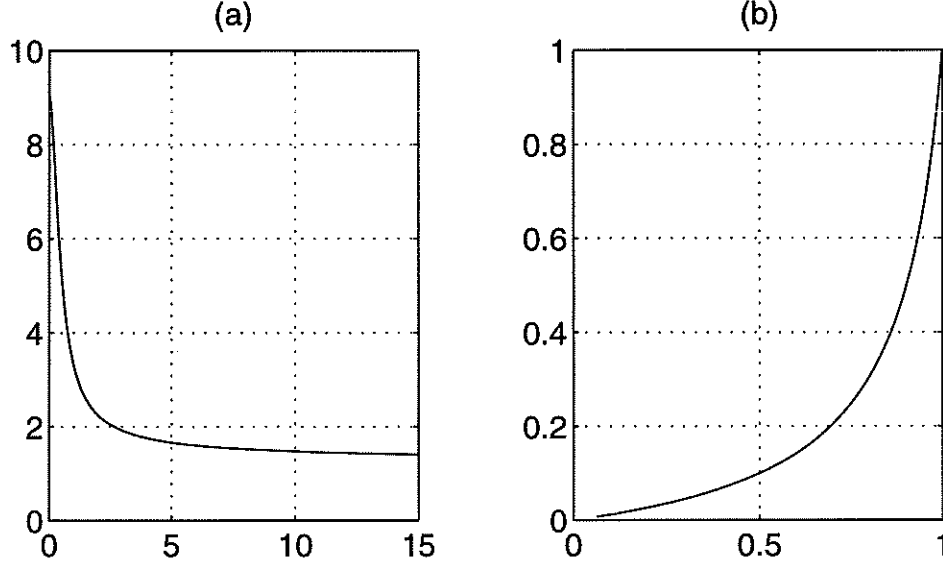


FIG. 1. a) Dependence of  $\alpha_M$  on  $C_1^{-1}$ . b) Dependence of the convergence rate of the method with  $M = M_{K+1}$  on that of the  $M = M_K$ .

Thus for very large values of  $C_1$ , we achieve large acceleration (up to nine times fewer steps need to be taken), while for small  $C_1$  the speed-up is negligible. In other words, the gain from using the more expensive prolongator smoother is most significant where the convergence with the less expensive smoother is slow. The dependence of  $\alpha_M$  on the value of  $C_1^{-1}$  is shown in Figure 1(a). Figure 1(b) depicts the dependence of the rate of convergence bound for the  $M = M_{K+1}$  on that of  $M = M_K$ . Computational complexity aspects will be discussed in section 5.  $\square$

*Remark 2.11 (preconditioning).* In order to use Algorithm 2.1 as a preconditioner of the conjugate gradients method, one needs to ensure that the error propagation operator of the iterative method is  $A$ -symmetric. As  $M$ ,  $M'$ , and  $A$  commute and are symmetric,  $M$  and  $M'$  are  $A$ -symmetric. Therefore the method employing the same presmoothen and postsmoother defined in two steps by  $\mathbf{y} \leftarrow S_M(\mathbf{x}, \mathbf{b})$ ;  $\mathbf{x} \leftarrow S_{M'}(\mathbf{y}, \mathbf{b})$  has an  $A$ -symmetric positive semidefinite error propagation operator

$$MM'(I - MP(P^T A_M P)^+ P^T M A) MM'.$$

Since  $\varrho(M), \varrho(M') \leq 1$ , Theorem 2.5 yields

$$(23) \quad \|MM'(I - MP(P^T A_M P)^+ P^T M A) MM'\|_A \leq (1 - C_2)^{1/2},$$

where  $C_2$  is given by (7). Let  $B$  denote one step of the iterative method for (1), having the error propagation operator (23), started from zero approximation. Then it follows from (23) by well-known arguments that the relative condition number  $\text{cond}(A, B)$  is bounded by  $\frac{1 + \sqrt{1 - C_2}}{C_2}$ .  $\square$

*Example 2.12.* To illustrate the theory developed in this section, consider simple Poisson equation: for given  $f \in H_0^{-1}([0, 1])$ , find  $u \in H_0^1([0, 1])$  such that

$$(u', v')_{L^2([0, 1])} = f(v) \quad \forall v \in H_0^1([0, 1]).$$

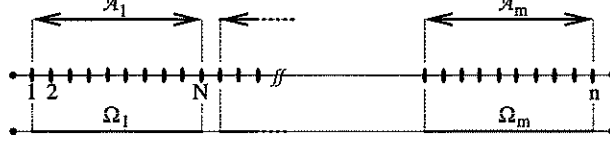


FIG. 2. Simplest one-dimensional aggregates:  $\mathcal{A}_1 = \{1, \dots, N\}$ ,  $\mathcal{A}_2 = \{N + 1, \dots, 2N\}$ , etc.

The model problem is discretized by P1 elements on a uniform grid of meshsize  $h = \frac{1}{mN+1}$ . We assume the standard scaling of the finite element basis,  $\|\varphi_i\|_{L^\infty} = 1$ . Such discretization leads to a system (1) of  $n = mN$  linear algebraic equations, each equation corresponding to one unconstrained node in the interval  $(0, 1)$ .

To define the  $n \times m$  tentative prolongator  $P$ , we create disjoint aggregates  $\{\mathcal{A}_i\}_{i=1}^m$  by grouping  $N$  neighboring nodes as shown in Figure 2. The  $j$ th column of  $P$  corresponds to disaggregation of  $j$ th coarse-level variable into all fine-level variables of the aggregate  $\mathcal{A}_j$ , i.e.,  $P_{ij} = 1$  for all  $j \in \mathcal{A}_i$ , zeros otherwise. That is,

$$P = \begin{pmatrix} 1 & \cdot & & & & & \\ 1 & \cdot & & & & & \\ \cdot & \cdot & & & & & \\ 1 & \cdot & & & & & \\ & 1 & \cdot & & & & \\ & & 1 & \cdot & & & \\ & & \cdot & \cdot & \cdot & & \\ & & \cdot & \cdot & \cdot & \cdot & \\ & & \cdot & \cdot & \cdot & \cdot & \\ & & \cdot & \cdot & \cdot & \cdot & \\ & & \cdot & \cdot & \cdot & \cdot & 1 \\ & & & & & & \cdot \\ & & & & & & \cdot \\ & & & & & & \cdot \\ & & & & & & \cdot \\ & & & & & & 1 \end{pmatrix}.$$

Consider a finite element interpolator  $\Pi : \mathbf{x} = (x_1, \dots, x_n)^T \mapsto \sum_i x_i \varphi_i$ . The prolongator  $P$ , applied to a vector  $\mathbf{v} = (v_1, \dots, v_m)^T$ , returns the value  $v_i$  in all the variables of the aggregate  $\mathcal{A}_i$ . Hence, for the corresponding finite element function,

$$(24) \quad \Pi P \mathbf{v} = v_i \text{ on } \Omega_i,$$

where  $\Omega_i$  is the subinterval of  $[0, 1]$  corresponding to the aggregate  $\mathcal{A}_i$ , see Figure 2.

Let  $H$  denote the length of the intervals  $\Omega_i$ . Verification of (3) consists in a straightforward application of the scaled Poincaré inequality on the subintervals  $\Omega_i$ ,

$$(25) \quad \min_{q \in \mathbb{R}} \|\Pi u - q\|_{L^2(\Omega_i)} \leq CH |u|_{H^1(\Omega_i)} \quad \forall u \in H^1(\Omega_i),$$

and the equivalence of discrete and continuous  $L^2$ -norms for finite element functions,

$$(26) \quad ch^{-1} \|\Pi \mathbf{u}\|_{L^2(\Omega_i)}^2 \leq \|\mathbf{u}\|_{l^2(\Omega_i)}^2 \equiv \sum_{j \in \mathcal{A}_i} u_j^2 \leq Ch^{-1} \|\Pi \mathbf{u}\|_{L^2(\Omega_i)}^2.$$

From (24), (25), and (26), it follows that for every  $\mathbf{u} \in \mathbb{R}^n$  there is a coarse-level vector  $\mathbf{v} = (v_1, \dots, v_m)^T$  such that

$$\|\mathbf{u} - P \mathbf{v}\|^2 = \sum_{i=1}^m \|\mathbf{u} - P \mathbf{v}\|_{l^2(\Omega_i)}^2 \leq Ch^{-1} \sum_{i=1}^m \|\Pi \mathbf{u} - v_i\|_{L^2(\Omega_i)}^2$$

$$\begin{aligned}
&= Ch^{-1} \sum_{i=1}^m \min_{q_i \in \mathbb{R}} \|\Pi \mathbf{u} - q_i\|_{L^2(\Omega_i)}^2 \leq C \frac{H^2}{h} \sum_{i=1}^m |\Pi \mathbf{u}|_{H^1(\Omega_i)}^2 \\
&\leq C \frac{H^2}{h} |\Pi \mathbf{u}|_{H^1([0,1])}^2.
\end{aligned}$$

Therefore, as  $\varrho(A) \leq Ch^{-1}$  and  $|\Pi \mathbf{u}|_{H^1([0,1])} = \|\mathbf{u}\|_A$ , it follows that there is a mapping  $Q_C : \mathbb{R}^n \rightarrow \text{Range}(P)$  such that

$$(27) \quad \|\mathbf{u} - Q_C \mathbf{u}\| \leq C \frac{H}{h \sqrt{\varrho(A)}} \|\mathbf{u}\|_A \quad \forall \mathbf{u} \in \mathbb{R}^n.$$

We use prolongator smoother  $M$  created by Algorithm 2.7, choosing  $d_M = \frac{1}{2} \frac{n}{m} \approx \frac{1}{2} \frac{H}{h}$ . By Lemma 2.8,  $\bar{\varrho}(A_M) \leq Cd_M^{-2} \varrho(A)$  which, together with (27), proves the approximation property (3) with a constant  $C_1$  independent of  $n$  and  $m$ .  $\square$

**3. Auxiliary coarse space for solids.** In this section we describe the construction of an auxiliary coarse space for problems of isotropic 3D elasticity with large jumps in Young modulus.

Let  $V^T$  be a conforming finite element space of the displacement field associated with a mesh  $\mathcal{T}$  on a Lipschitz domain  $\Omega$ , and  $\{\varphi_i\}_{i=1}^n$  be its basis. We assume there are three degrees of freedom (displacement components) per node, and the degrees of freedom are located only at the vertices of elements. Further, we assume that the elements support at least linear functions (i.e., for each element linear functions are contained in the space spanned by its finite element basis), the basis functions are scaled so that  $\|\varphi_i\|_{L^\infty} = 1$ ,  $|\varphi_i|_{H^1} \approx h_i$ , and the standard equivalence of discrete and continuous norms  $\|\sum \alpha_i \varphi_i\|_{L^2}^2 \approx \sum \alpha_i^2 h_i^3$  holds, where  $h_i$  denotes the local meshsize. It is obvious that standard P1 and Q1 elements conform to these assumptions.

Let  $V_0^T \subset V^T$  be the subspace of all finite element displacement fields subject to general single-point constraints. We may impose up to three linearly independent constraints per boundary node, in the form

$$(28) \quad \sum_{l=1}^3 \alpha_{kl} u_l(v) = 0, \quad \alpha_{kl} \in \mathbb{R}, \quad k = 1, \dots, 3,$$

where  $u_l(v)$  are components of the displacement field, and  $v \in \partial\Omega$ . We are interested in numerical solution of the following linear elasticity problem: Find a displacement field  $u \in V_0^T$  such that

$$a(u, v) = f(v) \quad \forall v \in V_0^T,$$

where

$$(29) \quad a(u, v) = \int_{\Omega} \left( \lambda \operatorname{div} u \operatorname{div} v + 2\mu \sum_{i,j} \varepsilon_{ij}(u) \varepsilon_{ij}(v) \right) dx.$$

Here  $\varepsilon$  is the strain tensor,  $\varepsilon_{ij}(u) = \frac{1}{2}(\partial_i u_j + \partial_j u_i)$ , and  $\lambda > 0$ ,  $\mu > 0$  are the Lamé coefficients. The Lamé coefficients can be expressed in terms of the Poisson ratio  $\nu$  and the Young modulus  $E$  as follows:

$$(30) \quad \mu = \frac{E}{1 + \nu} \quad \text{and} \quad \lambda = \frac{E\nu}{(1 + \nu)(1 - 2\nu)}.$$

The standard finite element discretization of the above bilinear form leads to a positive definite global stiffness matrix  $A_{\mathcal{T},0}$ . This matrix is obtained from the unconstrained global stiffness matrix  $A_{\mathcal{T}} = \{a(\varphi_i, \varphi_j)\}_{i,j=1}^n$  by eliminating some degrees of freedom using (28). We assume that the constrained degrees of freedom are chosen so that the following is satisfied: Each constrained degree of freedom on a node can be expressed as a linear combination of free degrees of freedom with coefficients bounded uniformly with respect to the node index. In other words, denoting  $S(v)$  and  $F(v)$  the index set of constrained and free degrees of freedom on node  $v$ , respectively, we assume that the single-point constraints (28) are transformed into

$$(31) \quad u_i = \sum_{j \in F(v)} \beta_{ij} u_j, \quad i \in S(v),$$

with coefficients  $|\beta_{ij}| \leq C_\beta$ . Here  $i$  and  $j$  are indices in the global numbering of degrees of freedom of the matrix  $A_{\mathcal{T}}$ . This can be done, for example, as follows. First, for each node where the boundary condition (28) is imposed, the Gauss–Jordan elimination with row pivoting is applied to the matrix  $\{\alpha_{ki}\}_{k,i=1}^3$  of constraints (28). Then degrees of freedom associated with the pivots are chosen to be the constrained degrees of freedom and are eliminated from the global stiffness matrix. In this case  $C_\beta \leq 2$ .

Let  $S$  denote the set of all constrained degrees of freedom,  $S = \cup_{v \in \mathcal{T}} S(v)$ , and similarly let  $F$  be the set of all free degrees of freedom  $F = \cup_{v \in \mathcal{T}} F(v)$ . We introduce a one-to-one mapping

$$(32) \quad N : F \rightarrow \{1, \dots, n_f \equiv \text{card}(F)\},$$

which establishes the index correspondence between the free degrees of freedom of  $A_{\mathcal{T}}$  and the unknowns of  $A_{\mathcal{T},0}$ . Let us note that the constrained stiffness matrix  $A_{\mathcal{T},0}$  can be interpreted as a Gram matrix  $\{a(\phi_i, \phi_j)\}_{i,j=1}^{n_f}$  with a modified finite element basis

$$(33) \quad \phi_{N(j)} = \varphi_j + \sum_{i \in S(v)} \beta_{ij} \varphi_i, \quad j \in F(v),$$

where the coefficients  $\beta_{ij}$  are given by (31). This basis is obtained from the requirement that the basis in (31) satisfies

$$\sum_{i=1}^3 v_i \varphi_i = \sum_{i \in F} v_i \phi_i.$$

We define matrix  $D$  as follows:

$$(34) \quad D_{ij} = \begin{cases} (A_{\mathcal{T},0})_{ij} & \text{if } i \text{ and } j \text{ are associated with the same node, i.e.,} \\ & i, j \in N(F(v)) \text{ for some } v \in \mathcal{T}, \\ 0 & \text{otherwise.} \end{cases}$$

This matrix is block diagonal when a suitable ordering of degrees of freedom is used. We will formulate the method for the following scaled matrix:

$$(35) \quad A = D^{-1/2} A_{\mathcal{T},0} D^{-1/2}.$$

This is motivated by the need to accommodate variations of coefficients in the equation and makes it possible to achieve invariance of the algorithm with respect to a change

of spatial coordinates in (29). This transformation also reduces the spectral condition number [18, 14].

Let  $\Omega_i, i = 1, \dots, n_s$ , be a system of closed disjoint subdomains of  $\Omega$  such that each subdomain is a simply connected aggregate of elements, and every node of the mesh belongs to exactly one subdomain. In other words, the union of  $\Omega_i$ s cover the set of all nodes, but it does not cover the whole domain—there is a layer one element wide between the neighboring subdomains. We use  $F_i$  and  $S_i$  to denote the set of all free and constrained degrees of freedom on subdomain  $\Omega_i$ , respectively.

On each subdomain  $\Omega_i$ , we define the space of rigid body modes

$$(36) \quad R_i = \{u(\mathbf{x}) = C\mathbf{x} + \mathbf{c}, \quad \mathbf{x} \in \Omega_i\},$$

where  $C$  is an arbitrary antisymmetric  $3 \times 3$  matrix and  $\mathbf{c} \in \mathbb{R}^3$  is a constant vector. To construct the auxiliary coarse space, we need a basis of  $R_i$ . As a computationally convenient example of a basis in  $R_i$ , we suggest  $\{f^{ij}(\mathbf{x}), \mathbf{x} = [x_1, x_2, x_3] \in \Omega_i\}_{j=1}^6$  given by

$$(37) [f^{i1}, f^{i2}, f^{i3}, f^{i4}, f^{i5}, f^{i6}] = \begin{bmatrix} -x_2 + x_2^0 & -x_3 + x_3^0 & 0 & 1 & 0 & 0 \\ x_1 - x_1^0 & 0 & -x_3 + x_3^0 & 0 & 1 & 0 \\ 0 & x_1 - x_1^0 & x_2 - x_2^0 & 0 & 0 & 1 \end{bmatrix},$$

where  $\mathbf{x}^0 = [x_1^0, x_2^0, x_3^0]$  is some fixed point in  $\Omega_i$ .

**ALGORITHM 3.1** (tentative prolongator).

*For every domain  $\Omega_i$  and for  $j = 1, \dots, 6$ ,*

1. *express  $f^{ij}$  as a linear combination of the basis of the unconstrained space  $V^T$  by*

$$f^{ij}(\mathbf{x}) = \sum_k c_k^{ij}(\varphi_k|_{\Omega_i});$$

2. *generate  $\mathbf{d}^{ij} \in \mathbb{R}^{n_f}$  by  $d_{N(k)}^{ij} = c_k^{ij} \quad \forall k \in F_i$ , where mapping  $N$  was defined in (32);*
3. *interpret vector  $D^{1/2}\mathbf{d}^{ij}$  as  $6(i-1) + j$ th column of the tentative prolongator  $P$ ;*
4. *for each subdomain  $\Omega_i$ , orthonormalize the associated columns of  $P$  (that is, columns  $6(i-1) + j, j = 1, \dots, 6$ ).*

Note that under our assumptions on the basis  $\{\varphi_i\}$  the coefficients  $c_k^{ij}$  are nodal values of the vector function  $f^{ij}$  at the grid points. But the algorithm in this form can be applied to more general bases (e.g., unscaled bases or high-order elements). Results given in the next section can be easily extended to such cases.

*Remark 3.2.* The construction of the tentative prolongator  $P$  suitable for solving second-order scalar problems appeared in [21]. It can be obtained by simplification of Algorithm 3.1 as follows: On aggregate  $i$ , instead of the local basis of the rigid body modes  $\{f^{ij}(x)\}_{j=1}^6$  given by (37), we use a single function  $f^{i1}(x) \equiv 1$ .

This leads to obvious simplifications in the algorithm. These simplifications include replacing all the loops over the 6 rigid body mode basis by a single operation. This choice also implies that the columns of  $P$  will always be orthogonal, and the orthonormalization step 4 of Algorithm 3.1 reduces to a simple scaling by the number of nodes in each aggregate.  $\square$

**4. Verification of the weak approximation property.** For the tentative coarse space given by Algorithm 3.1 we will show the weak approximation condition (3) with a constant independent of the boundary conditions, the domain  $\Omega$ , and the magnitude of the jumps in  $E$ , provided the subdomains  $\Omega_i$  are suitably aligned with the jumps. We need to introduce additional notation and assumptions on the triangulation and subdomain decomposition.

**DEFINITION 4.1** (see [9]). *Suppose a domain  $\omega$  has diameter  $d$  and is star-shaped with respect to a ball  $B$ , i.e.,  $\forall x \in \omega$ , the closed convex hull of  $\{x\} \cup B$  is a subset of  $\omega$ . Let  $\varrho_{\max} = \sup\{\varrho : \omega \text{ is star-shaped with respect to a ball of radius } \varrho\}$ . Then the chunkiness parameter of  $\omega$  is defined by*

$$\gamma(\omega) = \frac{d}{\varrho_{\max}}.$$

**ASSUMPTION 4.2.**

1. Each  $\Omega_i$  can be mapped onto a unit cube  $\hat{\Omega}$  by a mapping  $F_i : \Omega_i \rightarrow \hat{\Omega}$  that satisfies

$$(38) \quad c_F \frac{1}{H_i} \leq \|\partial F_i(x)\| \leq C_F \frac{1}{H_i} \quad \forall x \in \Omega_i$$

where  $\|\cdot\|$  is a  $3 \times 3$  operator matrix norm. In other words,  $\Omega_i$  is a shape-regular domain of characteristic size  $H_i$ .

2. There is about the same number of elements in each subdomain. More specifically, denoting the characteristic number of elements per subdomain by  $N_{es}$ , we require

$$(39) \quad c_H N_{es}^{1/3} \leq H_i/h_i \leq C_H N_{es}^{1/3}.$$

A bounded number of subdomains may violate this requirement in the sense that the number of elements they contain may be smaller.

3. Each subdomain  $\Omega_i$  is a union of at most  $k_\Omega$  star-shaped domains  $\omega_j^i$  with uniformly bounded chunkiness parameters  $\gamma(\omega_j^i) < \gamma_0$  such that

$$\mu(\omega_{k+1}^i \cap (\cup_{j=1}^k \omega_j^i)) \geq c_0 \min(\mu(\omega_{k+1}^i), \mu(\cup_{j=1}^k \omega_j^i)), \quad k < k_\Omega.$$

4. The triangulation  $\mathcal{T}$  is shape-regular and is quasi-uniform with a characteristic element size  $h_i$  on each subdomain  $\Omega_i$ .
5. The Poisson ratio satisfies  $0 < \nu_1 \leq \nu(x) \leq \nu_2 < 0.5$  and the Young modulus  $E$  is almost constant on each subdomain in the sense that there exist positive constants  $c_E$  and  $C_E$  independent of the subdomain index and a constant  $\bar{E}_i > 0$  such that, on  $\Omega_i$ ,  $c_E \bar{E}_i \leq E \leq C_E \bar{E}_i$ .
6. If  $\Omega_i$  and  $\Omega_j$  are neighboring subdomains (in the sense that for some element  $T \in \mathcal{T}$  it holds that  $\partial T \cap \partial \Omega_i \neq \emptyset$  and  $\partial T \cap \partial \Omega_j \neq \emptyset$ ) and  $\bar{E}_i \gg \bar{E}_j$ , we assume that there is a jump in  $E$  that occurs at  $\partial \Omega_i$ . In other words, the discontinuity is located on the boundary of the subdomain with a larger Young modulus.

The purpose of Assumption 4.2, item 6, is to ensure for the basis function  $\varphi_j$  associated with a node  $v \in \Omega_i$  to satisfy

$$(40) \quad a(\varphi_j, \varphi_j) \approx h_i \bar{E}_i.$$

If Assumption 4.2, item 6, were not satisfied, the basis functions corresponding to the nodes on  $\partial\Omega_j$  adjacent to a subdomain  $\Omega_i$  with  $\bar{E}_i \gg \bar{E}_j$  could violate (40).

*Remark 4.3.* In an attempt to satisfy the geometrical aspects of Assumption 4.2, we use a greedy-type algorithm in practical implementation. It is known that a straightforward greedy algorithm may produce isolated points and subdomains of measure zero. The modified greedy algorithm we will use (see [10, Chapter 3]) does not suffer from this behavior and tends to satisfy Assumption 4.2.  $\square$

The following lemma will be useful in proving the weak approximation property later in this section.

LEMMA 4.4. *Under Assumption 4.2, items 1 and 3, it holds that*

$$\inf_{w \in R_i} \|u - w\|_{[L^2(\Omega_i)]^3}^2 \leq CH_i^2 \int_{\Omega_i} \sum_{i,j=1}^3 \varepsilon_{ij}(u)^2 dx \quad \forall u \in [H^1(\Omega_i)]^3,$$

where  $C$  depends on  $\gamma_0$ ,  $c_0$ ,  $k_\Omega$ .

*Proof.* It is well known [15] that for a star-shaped domain  $\omega$ , Korn's constant  $K(\omega)$  on the factor space modulo rigid body modes  $R$ ,

$$K(\omega)^{-1} = \inf_u \frac{\int_\omega \sum_{i,j=1}^3 \varepsilon_{ij}(u)^2 dx}{|u|_{[H^1(\omega)]^3/R}},$$

can be controlled in terms of the chunkiness parameter  $\gamma(\omega)$ . Furthermore, for two Lipschitz domains  $\omega_1$  and  $\omega_2$ , Korn's constant on  $\omega_1 \cup \omega_2$  can be estimated [12] as

$$K(\omega_1 \cup \omega_2) \geq K(\omega_1) + K(\omega_2) + \frac{\min(\mu(\omega_1), \mu(\omega_2))}{\mu(\omega_1 \cap \omega_2)} (\sqrt{K(\omega_1)} + \sqrt{K(\omega_2)})^2,$$

where  $\mu$  denotes the Lebesgue measure. This, together with the assumptions, implies that  $K(\Omega_i)$  depends only on  $\gamma_0$ ,  $c_0$ , and  $k_\Omega$ . The scaled Poincaré inequality completes the proof.  $\square$

For  $\Delta \subset \Omega$ , we will use  $a_\Delta$  to denote the bilinear form defined by taking the integral in (29) over  $\Delta$ . The following lemma will be useful in the proof of the weak approximation property (Lemma 4.6).

LEMMA 4.5. *Let  $D$  be the matrix defined by (34),  $D_1 = \text{diag}(A_{T,0})$  and  $D_2 = \text{diag}(\{a(\varphi_{N-1(i)}, \varphi_{N-1(j)})\}_{i,j=1}^{n_f})$ . Then, by Assumption 4.2, items 3 and 4,  $D, D_1$ , and  $D_2$  are spectrally equivalent with constants of equivalence depending only on aspect ratios of elements.*

*Proof.* As with a suitable (re)ordering, every matrix in question is either diagonal or block diagonal, we can prove the spectral equivalence node by node (i.e., block by block). For convenience, we shall omit node indices. That is, throughout this lemma, we use symbols  $D, D_1$ , and  $D_2$  to denote appropriate blocks corresponding to a node, and  $F \equiv F(v), S \equiv S(v)$ . Thus, our blocks corresponding to a node  $v$  are defined by  $D = \{a(\phi_i, \phi_j)\}_{i,j \in N(F)}$ ,  $D_1 = \text{diag}(D)$ ,  $D_2 = \text{diag}(\{a(\varphi_i, \varphi_j)\}_{i,j \in F})$ ; see (33). Let  $\mathcal{S}$  denote the (shared) support of basis functions  $\phi_{N(i)}, \varphi_i, i \in F$ , and  $T \in \mathcal{S}$  an element adjacent to the node  $v$ .

Denoting the characteristic Young modulus on  $T$  by  $E_T$ , Korn's inequality, together with boundedness of  $a(\cdot, \cdot)$ , gives

$$a_T \left( \sum_{i \in F \cup \mathcal{S}} c_i \varphi_i, \sum_{j \in F \cup \mathcal{S}} c_j \varphi_j \right) \approx E_T \sum_{i \in F \cup \mathcal{S}} c_i^2 |\varphi_i|_{H^1(T)}^2 \approx \sum_{i \in F \cup \mathcal{S}} c_i^2 a_T(\varphi_i, \varphi_i),$$



where the constants of equivalence depend only on the shape of the elements. Summing over all elements adjacent to node  $v$ , we obtain

$$(41) \quad a_S \left( \sum_{i \in SUF} c_i \varphi_i, \sum_{i \in SUF} c_i \varphi_i \right) \approx \sum_{i \in SUF} c_i^2 a_S(\varphi_i, \varphi_i) \approx E_S^2 h \sum_{i \in SUF} c_i^2,$$

where  $h$  is the local meshsize, and  $E_S^2 = \max_{T \in \mathcal{S}} E_T^2$ . By definition of  $D$  and (33), for  $\mathbf{w} = \{w_{N(i)}\}_{i \in F}$

$$\begin{aligned} & \mathbf{w}^T D \mathbf{w} \\ &= a \left( \sum_{j \in F} w_{N(j)} \varphi_j + \sum_{i \in S} \left( \sum_{j \in F} w_{N(j)} \beta_{ij} \right) \varphi_i, \sum_{j \in F} w_{N(j)} \varphi_j + \sum_{i \in S} \left( \sum_{j \in F} w_{N(j)} \beta_{ij} \right) \varphi_i \right). \end{aligned}$$

Thus, denoting  $\delta_i = w_{N(i)}$  for  $i \in F$  and  $\delta_i = \sum_{j \in F} w_{N(j)} \beta_{ij}$  for  $i \in S$ , we have

$$\mathbf{w}^T D \mathbf{w} \approx \sum_{i \in F \cup S} E_S^2 h \delta_i^2.$$

As  $0 \leq |\beta_{ij}| \leq \text{card}(S)$ ,  $\mathbf{w}^T D \mathbf{w} \approx E_S^2 h \mathbf{w}^T \mathbf{w} \approx \mathbf{w}^T D_2 \mathbf{w}$ .

In order to prove that  $D_1 \approx D_2$ , it suffices to show that

$$a \left( \varphi_j + \sum_{i \in S} \beta_{ji} \varphi_i, \varphi_j + \sum_{i \in S} \beta_{ji} \varphi_i \right) \approx E_S^2 h \quad \text{for } j \in F.$$

From (41) and  $|\beta_{ij}| \leq \text{card}(S)$  it follows that

$$a \left( \varphi_j + \sum_{i \in S} \beta_{ij} \varphi_i, \varphi_j + \sum_{i \in S} \beta_{ij} \varphi_i \right) \approx a(\varphi_j, \varphi_j) + \sum_{i \in S} \beta_{ij}^2 a(\varphi_i, \varphi_i) \approx E_S^2 h,$$

completing the proof.  $\square$

Before we turn to proving the weak approximation property, we introduce some additional notation. Recall that  $n_f = \text{card}(F)$  is the number of all free degrees of freedom, and  $\{\varphi_i\}_{i=1}^{n_f}$  and  $\{\phi_i\}_{i=1}^{n_f}$  are the finite element bases of the constrained and unconstrained finite element spaces, respectively. Consider the index set  $\mathcal{I} \subset \{1, \dots, n = \text{card}(F \cup S)\}$ .

For the vector  $\mathbf{x} \in \mathbb{R}^n$  we define the discrete  $l^2$ -norm

$$\|\mathbf{x}\|_{l^2(\mathcal{I})} = \left( \sum_{i \in \mathcal{I}} x_i^2 \right)^{1/2}.$$

The subspace of all vectors  $\mathbf{x} \in \mathbb{R}^n$  such that  $x_i = 0 \forall i \notin \mathcal{I}$  will be denoted by  $V(\mathcal{I})$ . Let us define the finite element interpolators

$$\begin{aligned} \Pi_0 : \mathbf{u} \in \mathbb{R}^{n_f} &\mapsto \sum_{i=1}^{n_f} u_i \phi_i, \\ \Pi_0^i : \mathbf{u} \in V(F_i) \subset \mathbb{R}^n &\mapsto \sum_{i \in N(F_i)} u_i \phi_i, \\ \Pi : \mathbf{u} \in \mathbb{R}^n &\mapsto \sum_{i \in F \cup S} u_i \varphi_i, \\ \Pi^i : \mathbf{u} \in V(F_i \cup S_i) \subset \mathbb{R}^n &\mapsto \sum_{i \in F_i \cup S_i} u_i \varphi_i. \end{aligned}$$

The inverses of these interpolators are well defined on their respective ranges.

Let  $P_{R_i} : [H^1(\Omega_i)]^3 \rightarrow R_i$  be the  $L^2$ -orthogonal projection onto the space  $R_i$  of rigid body modes on  $\Omega_i$ . We define the linear operator  $Q_i : [H^1(\Omega_i)]^3 \rightarrow \text{Range}(\Pi_0^i)$  in the following four steps:

1.  $u \in [H^1(\Omega_i)]^3 \mapsto v = P_{R_i} u \in R_i$ .
2.  $v \mapsto \mathbf{w} = (\Pi^i)^{-1} v \in V(F_i \cup S_i)$ .
3.  $\mathbf{w} \mapsto \mathbf{w}^c \in V(F_i)$  by  $w_j^c = w_j$  if  $j \in F_i$ , zero otherwise.
4. Set  $Q_i u = \Pi_0^i \mathbf{w}^c$ .

Finally, let us define the mapping  $Q : \mathbb{R}^{n_f} \rightarrow \mathbb{R}^{n_f}$  by

$$Q = (\Pi_0)^{-1} \left( \sum_{i=1}^{n_s} Q_i \right) \Pi_0.$$

LEMMA 4.6 (weak approximation property). *Let  $\|\cdot\|$  denote the Euclidean norm in  $\mathbb{R}^{n_f}$ . Under Assumption 4.2 it holds that*

$$(42) \quad \|\mathbf{u} - D^{1/2} Q D^{-1/2} \mathbf{u}\| \leq C N_{es}^{1/3} \|\mathbf{u}\|_A \quad \forall \mathbf{u} \in \mathbb{R}^{n_f},$$

where the constant  $C$  depends only on the constants from Assumption 4.2. Moreover, for the prolongator  $P$  generated by Algorithm 3.1, we have

$$(43) \quad \text{Range}(D^{1/2} Q D^{-1/2}) = \text{Range}(P).$$

*Proof.* The proof of (43) follows immediately from the construction of  $P$  and  $Q$ . Let us prove (42). Setting  $\mathbf{u} = D^{1/2} \mathbf{v}$ , we have  $\|\mathbf{u} - D^{1/2} Q D^{-1/2} \mathbf{u}\|^2 = \|D^{1/2} (I - Q) \mathbf{v}\|^2$ . Due to Lemma 4.5, we may replace  $D$  by the spectrally equivalent matrix  $D_2$ . Consequently, owing to (40), we can write

$$(44) \quad \begin{aligned} \|\mathbf{u} - D^{1/2} Q D^{-1/2} \mathbf{u}\|^2 &\leq C \|D_2^{1/2} (I - Q) \mathbf{v}\|^2 \\ &\leq C \sum_{i=1}^{n_s} \bar{E}_i h_i \|\mathbf{v} - (\Pi_0^i)^{-1} Q_i \Pi_0^i \mathbf{v}\|_{L^2(F_i)}^2. \end{aligned}$$

The operator  $(\Pi_0^i)^{-1} Q_i \Pi_0^i \mathbf{v}$  returns the nodal values of  $P_{R_i} \Pi_0^i \mathbf{v}$  in  $F_i$  (the unconstrained degrees of freedom of  $\Omega_i$ ). For

$$\mathbf{x} = (\Pi_0^i)^{-1} Q_i \Pi_0^i \mathbf{v} \quad \text{and} \quad \mathbf{y} = (\Pi^i)^{-1} P_{R_i} \Pi_0^i \mathbf{v}$$

we have  $y_j = x_j \forall j \in F_i$ . For the same reason,  $\|\mathbf{v}\|_{L^2(F_i)} = \|(\Pi^i)^{-1} \Pi_0^i \mathbf{v}\|_{L^2(F_i)}$ . Thus,

$$\begin{aligned} \|\mathbf{v} - (\Pi_0^i)^{-1} Q_i \Pi_0^i \mathbf{v}\|_{L^2(F_i)}^2 &= \|(\Pi^i)^{-1} (I - P_{R_i}) \Pi_0^i \mathbf{v}\|_{L^2(F_i)}^2 \\ &\leq \|(\Pi^i)^{-1} (I - P_{R_i}) \Pi_0^i \mathbf{v}\|_{L^2(F_i \cup S_i)}^2 \\ &\leq C h_i^{-3} \| (I - P_{R_i}) \Pi_0^i \mathbf{v} \|_{[L^2(\Omega_i)]^3}^2. \end{aligned}$$

Substituting the last estimate into (44) and using Lemma 4.4 and (39), we obtain

$$(45) \quad \begin{aligned} \|\mathbf{u} - D^{1/2} Q D^{-1/2} \mathbf{u}\|^2 &\leq C \sum_{i=1}^{n_s} \bar{E}_i \left( \frac{H_i}{h_i} \right)^2 \int_{\Omega_i} \sum_{k,l=1}^3 \varepsilon_{kl} (\Pi_0^i \mathbf{v})^2 dx \\ &\leq C N_{es}^{2/3} a(\Pi_0 \mathbf{v}, \Pi_0 \mathbf{v}) \\ &= C N_{es}^{2/3} \langle A_{T,0} \mathbf{v}, \mathbf{v} \rangle = C N_{es}^{2/3} \langle A \mathbf{u}, \mathbf{u} \rangle, \end{aligned}$$

which completes the proof.  $\square$

**5. Main result.** We are now ready to formulate and prove the convergence theorem.

**THEOREM 5.1.** *Let the tentative prolongator  $P$  be given by Algorithm 3.1 applied to a system of subdomains  $\{\Omega_i\}_{i=1}^m$  satisfying Assumption 4.2. Let the prolongator smoother  $M$  be defined by Algorithm 2.7 with  $d_M$  satisfying*

$$(46) \quad c_N N_{es}^{1/3} \leq d_M \leq C_N N_{es}^{1/3}.$$

Then the error  $\mathbf{e}_i^M$  satisfies

$$(47) \quad \|\mathbf{e}_i^M\|_A^2 \leq (1 - C)^i \|\mathbf{e}_0\|_A^2.$$

Constant  $C$  depends on  $C_\rho$ , maximal aspect ratio of elements, constants from Assumption 4.2, (46), and is independent of  $H_i$ ,  $h_i$ ,  $\bar{E}_i$ ,  $\Omega$ , and boundary conditions. Moreover, the coarse-level matrix and the smoothed prolongator  $MP$  have their number of nonzero entries per row bounded uniformly with respect to both  $n$  and  $N_{es}$ .

*Proof.* As  $\deg(M) \leq c_N \frac{1}{2} N_{es}^{1/3}$ , it follows from Lemmas 4.6 and 2.8 that the approximation property (3) holds with a constant  $C_1$  independent of  $m$  and  $n$ . The optimal convergence result follows from Theorem 2.5.

Let us show that the number of nonzero entries per row of the coarse-level matrix  $A_c = (MP)^T A (MP)$  is bounded uniformly with respect to  $n$ ,  $N_{es}$ . It is easy to see that  $[A_c]_{ij}$  can be nonzero only if  $\text{supp}(\Pi_0 M P e^i) \cap \text{supp}(\Pi_0 M P e^j) \neq \emptyset$ , where  $\mathbf{e}^i$  is the  $i$ th canonical basis vector of  $\mathbb{R}^m$ . Clearly,  $\text{supp}(\Pi_0 P e^i)$  is the domain  $\Omega_i$  with one belt of surrounding elements added. Bounded overlaps of such supports are obvious. The smoother  $M$  adds at most  $\deg(M) \approx \frac{1}{2} N_{es}^{1/3} \approx \frac{1}{2} H_i/h_i$  strips of elements. As subdomains  $\Omega_i$  are assumed shape-regular with the “mesh diameter” of about  $H_i/h_i$  elements, each support has a nonempty intersection with only a bounded number of other supports.<sup>1</sup> The sparsity of  $MP$  follows.  $\square$

**THEOREM 5.2.** *Let the assumptions of Theorem 5.1 be fulfilled and the Cholesky factorization be used to solve the coarse-level problem. Then the optimal number of elements per subdomain is  $N_{es} \approx n^{1/2}$  and the system (1) can be solved to the level of truncation error in  $O(n^{7/6})$  operations.*

*Proof.* Operation counts in this proof make use of the fact that the matrices  $MP$  and  $P^T M^2 A P$  are sparse and we have to perform  $O(1)$  iterations. Components of the setup phase, and their respective costs in number of floating point operations, are

$$\begin{aligned} \text{Construction of MP:} & \quad O(\deg(M)n) = O(N_{es}^{1/3} n). \\ \text{Construction of coarse-level matrix:} & \quad O(n). \\ \text{Factorization of coarse-level matrix:} & \quad O((n/N_{es})^{7/3}). \end{aligned}$$

<sup>1</sup>The subdomains  $\Omega_i$  are shape-regular (see (38)) with characteristic size  $H_i$ , and the mesh on  $\Omega_i$  is quasi-uniform with characteristic meshsize  $h_i$ ,  $H_i/h_i \approx N_{es}^{1/3}$ . It follows from the shape regularity of  $\Omega_i$  that there is a ball  $B_i$  with diameter greater than  $cH_i$  inscribed in  $\Omega_i$ . The quasi-uniformity of the mesh assures that each line going through the center  $\mathbf{c}_i$  of  $B_i$  intersects at least  $kN_{es}^{1/3}$  elements inside  $B_i$ , where  $k$  is a constant independent of  $n, N_{es}$ . In other words,

$$(48) \quad \text{Each ball } B_i \text{ contains at least } kN_{es}^{1/3} \text{ belts of elements surrounding } \mathbf{c}_i.$$

By analogous reasoning, we can show that a line connecting  $\mathbf{c}_i$  with a node on  $\partial\Omega_i$  intersects at most  $kN_{es}^{1/3}$  elements. Further, two supports  $\text{supp}(\Pi_0 M P e^i)$ ,  $\text{supp}(\Pi_0 M P e^j)$  can intersect only if there is a path from  $\mathbf{c}_i$  to  $\mathbf{c}_j$  that intersects at most  $2(K + 1 + \deg(M)) \approx N_{es}^{1/3}$  elements. In other words,  $\mathbf{c}_j$  must be contained in the domain consisting of  $2(K + 1 + \deg(M)) \approx N_{es}^{1/3}$  strips of elements surrounding  $\mathbf{c}_i$  for the overlap to occur. From (48) it follows that the number of such centers  $\mathbf{c}_j$  is bounded uniformly with respect to both  $N_{es}$  and  $n$ .

The iterative phase consists of the following components:

Smoothing:	$O((\deg(M)n)) = O(N_{es}^{1/3}n)$ .
Prolongation, restriction, defect evaluation:	$O(n)$ .
Back substitution:	$O((n/N_{es})^{5/3})$ .

Summarizing, the total cost is:

$$\max \left( O(nN_{es}^{1/3}), O((n/N_{es})^{7/3}) \right).$$

Minimizing, we find that the optimal subdomain size is  $N_{es} = n^{1/2}$ . In that case, the total cost is of the order of  $n^{7/6}$ .  $\square$

*Remark 5.3* (choice of the degree of the prolongator smoother). Let  $N_d$  denote the average number of nodes per subdomain. Note that  $N_d \approx N_{es}$ . For computational purposes, we suggest choosing

$$d_M = \left\lfloor \frac{1}{2}(N_d^{1/3} - 1) \right\rfloor,$$

where  $\lfloor \cdot \rfloor$  denotes the truncation to the nearest smaller integer. This choice is motivated as follows. Let  $\mathbf{e}_i$  denote the  $i$ th canonical basis vector of  $\mathbb{R}^{6n_s}$ . Assume we have a uniform grid of a meshsize  $h$  and our subdomains are cubes of size  $H$ . Then  $N_d^{1/3} - 1 = H/h$ , and the choice of  $d_M$  assures that supports of coarse space basis functions  $\text{supp}(\Pi_0 M P \mathbf{e}^i)$ ,  $\text{supp}(\Pi_0 M P \mathbf{e}^j)$  overlap only if these basis functions correspond to the same subdomain or two adjacent subdomains.  $\square$

*Remark 5.4* (case without jumps in  $E$ ). If  $E \approx \bar{E}$  on  $\Omega$ , we can show that the weak approximation property (42) holds even for subdomains that do not satisfy Assumption 4.2.3. To this end, let  $\Omega^{ext}$ ,  $\Omega \subset \Omega^{ext}$ , be a sufficiently large domain. Let us consider the extension  $u_{ext} \in [H^1(\Omega^{ext})]^3$  of  $u \in [H^1(\Omega)]^3$  such that  $u_{ext} = u$  on  $\Omega$  and

$$(49) \quad a_{\Omega^{ext}}(u_{ext}, u_{ext}) \leq C(\Omega) a(u, u).$$

Such an extension exists owing to the  $H^1$  extension theorem [1] and Korn's inequality on the factorspace modulo rigid body modes on  $\Omega$ . For each subdomain  $\Omega_i$  let us consider a domain  $\Omega_i^{ext}$ ,  $\Omega_i \subset \Omega_i^{ext}$ , such that  $\Omega_i^{ext}$  satisfies Assumption 4.2, item 3,  $H_i$  is the characteristic size of  $\Omega_i^{ext}$  (in the sense of (38)), and overlaps of subdomains  $\Omega_i^{ext}$  are bounded. For example, we can choose  $\Omega_i^{ext}$  to be cubes. Then, following the proof of Lemma 4.4, we obtain

$$(50) \quad \bar{E} \inf_{w \in R_i} \|u - w\|_{L^2(\Omega_i)}^2 \leq C H_i^2 a_{\Omega^{ext}}(u_{ext}, u_{ext})$$

and the weak approximation property (42) can be proven with the constant  $C$  dependent on  $\Omega$ , provided that the argument (45) in the proof of Lemma 4.6 is replaced with

$$(51) \quad \begin{aligned} \|\mathbf{u} - D^{1/2} Q D^{-1/2} \mathbf{u}\|^2 &\leq C \sum_{i=1}^{n_s} \left( \frac{H_i}{h_i} \right)^2 a_{\Omega_i^{ext}}((\Pi_0 \mathbf{v})_{ext}, (\Pi_0 \mathbf{v})_{ext}) \\ &\leq C N_{es}^{2/3} a_{\Omega^{ext}}((\Pi_0 \mathbf{v})_{ext}, (\Pi_0 \mathbf{v})_{ext}) \\ &\leq C(\Omega) N_{es}^{2/3} a(\Pi_0 \mathbf{v}, \Pi_0 \mathbf{v}) \\ &= C(\Omega) N_{es}^{2/3} \langle A_{T,0} \mathbf{v}, \mathbf{v} \rangle \\ &= C(\Omega) N_{es}^{2/3} \langle A \mathbf{u}, \mathbf{u} \rangle. \end{aligned}$$

The convergence result obtained this way depends on the constant  $C(\Omega)$  from (49). This undesirable dependence can be eliminated if subdomains  $\Omega_i$  and  $\Omega_i^{ext}$  are chosen so that  $\Omega_i^{ext} \subset \Omega, i = 1, \dots, n_s$ .  $\square$

*Remark 5.5.* Both the method and the theory can easily be modified for the case of planar elasticity, where the optimal number of elements per subdomain is  $N_{es} \approx n^{2/5}$  and the resulting computational complexity is  $O(n^{1.2})$ .  $\square$

**6. Numerical experiments.** In this section, we present two sets of numerical experiments for the elasticity problem (29). Model experiments on a uniformly discretized cube validate the theory above, i.e., uniformity of the convergence with respect to a coarse-space size, boundary conditions, and jumps in coefficients.

The second set of experiments includes problems with jumps in coefficients that are not aligned with subdomains, randomly chosen Young moduli, and a real-life model of a turbine. The purpose of these experiments is to illustrate the potential of the method in situations when some of the assumptions of the theory are violated.

The stiffness matrices and rigid body modes for all the problems were generated by discretizing the linear elasticity problem (29) using CHEXA UAI/NASTRAN elements. We have used the current method as a conjugate gradient preconditioner and stopped the iteration process once the relative preconditioned residual satisfied

$$\left[ \frac{\langle BAe_i, Ae_i \rangle}{\langle BAe_0, Ae_0 \rangle} \text{cond}(B, A) \right]^{1/2} \leq 5 \cdot 10^{-5},$$

where  $B$  is the preconditioner and  $\text{cond}(B, A)$  is a condition number estimate computed at run time. The computational domains have been decomposed using a greedy algorithm that tends to generate nearly cubic subdomains of about the same size for regular meshes (for details, see [10, Chapter 3]).

Experiments in Tables 1, 2, 4, and 5 were performed on an IBM RS 6000/360. Due to memory requirements of a mesh with more than 120,000 degrees of freedom, we carried out the experiments with the turbine on a multiprocessor Silicon Graphics Power Challenge, using only one of its 90MHz R8000 CPUs.

In the table headers, we use the following symbols:

$n_s$	the number of subdomains.
$\text{deg}(M)$	prolongator smoother degree.
$Z$	fill-in of the coarse-level matrix (see the description below).
$N_{it}$	number of iterations.
$\rho$	rate of convergence = (relative residual after $N_{it}$ iterations) $^{1/N_{it}}$ .
cond	condition number estimate.
CPU	Setup CPU time + iteration CPU time (in seconds).

On the coarse level, there are six degrees of freedom associated with each subdomain. The coarse-level matrix is stored in a block-sparse format; the order of each block is 6. Block  $ij$  contains the information about the communication of the  $i$ th and  $j$ th subdomains. The number  $Z$  reported in tables is the average number of nonzero blocks per column of the coarse-level matrix.

*Uniformity of the convergence with respect to coarse-space size.* In order to verify the coarse-space size independent convergence, we have run two experiments with quite different numbers of subdomains. The computational domain was a uniformly discretized  $[0, 1] \times [0, 1] \times [0, 1]$  cube. We have prescribed zero Dirichlet boundary condition on one face of the cube and used Young modulus  $E = 1$  and Poisson ratio  $\nu = 0.3$ . The results are shown in Table 1.

TABLE 1  
*Uniformity of convergence with respect to coarse-space size.*

Cube: 9261 nodes, 27783 degrees of freedom, $E = \text{const}$ , $\nu = 0.3$							
Remark	$n_s$	$\text{deg}(M)$	$Z$	$N_{it}$	$T_{CPU}$	$\rho$	cond
Optimal degree of the prolongator smoother							
Large subd.	8	4	8	5	30 + 37	0.07	1.30
Small subd.	343	1	23	5	33 + 20	0.09	1.37
Nonoptimal degree of the prolongator smoother							
Large subd.	8	1	12	15	9 + 50	0.48	13.02
Small subd.	343	4	156	3	464 + 25	0.026	1.11

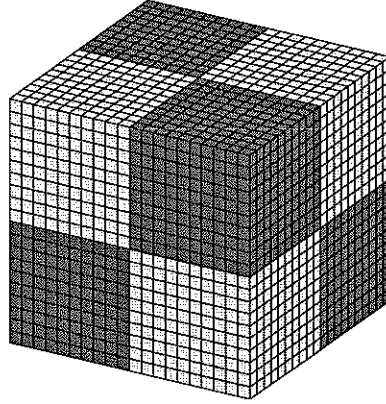


FIG. 3. *Jumps in  $E$ . Young modulus ( $E = E_1$ ) on dark subdomains;  $E = E_2 = 1 < E_1$  on light ones. All dark subdomains are visible.*

*Uniformity of the convergence with respect to jumps in Young modulus.* In order to demonstrate the uniform boundedness of the convergence with respect to jumps in coefficients, we have carried out two sets of numerical experiments. In the first set, the cube was subdivided into eight subdomains (see Figure 3). There is a greater Young modulus  $E = E_1$  on dark subdomains, while on the lighter subdomains  $E = E_2 = 1$ . Zero Dirichlet boundary condition was imposed at all corners of the lower face and the adjacent surface points. Results of experiments are summed up in Table 2. Only the experiments with 8 computational subdomains conform to Assumption 4.2; the other cases violate Assumption 4.2, item 6.

For the second set of experiments, the cube was decomposed into 27 smaller cubes ( $7 \times 7 \times 7$  nodes each). There is only one subdomain which is completely inside. We have chosen Young modulus  $E = E_1$  on this subdomain, and  $E = E_2$  elsewhere. This implies that the jumps have been aligned to meet the assumptions of our theory. Zero Dirichlet boundary condition was imposed at all corners of the lower face and at the adjacent surface points. Table 3 shows the results for a changing ratio  $E_1/E_2$ .

*Uniformity of the convergence with respect to boundary conditions.* This set of experiments, shown in Table 4, demonstrates independence of the convergence with respect to boundary conditions. The abbreviations used in the table stand for the following boundary conditions:

*Face BC:* Zero boundary condition on the lower face  $[0, 1] \times [0, 1] \times \{0\}$  of the cube.

TABLE 2

Uniformity of convergence with respect to jumps in Young modulus. Symbol \* indicates that the assumptions of the theory are not valid.

Cube: 9261 nodes, 27783 dfs, $\nu = 0.3$ , for $E$ see Fig. 3							
$E_1/E_2$	$n_s$	$\deg(M)$	Z	$N_{it}$	$T_{CPU}$	$\rho$	cond
10	8	4	8	6	31 + 68	0.141	1.75
10*	27	4	18	7	47 + 32	0.196	2.30
10*	343	1	23	5	30 + 19	0.125	1.50
100	8	4	8	8	30 + 85	0.231	3.54
100*	27	4	18	9	47 + 40	0.296	3.91
100*	343	1	23	6	31 + 23	0.146	1.80
1000	8	4	8	8	32 + 87	0.258	4.46
1000*	27	4	18	10	48 + 45	0.328	4.96
1000*	343	1	23	6	31 + 22	0.150	1.81

TABLE 3

Uniformity of convergence with respect to jumps in Young modulus.

Cube: 9261 nodes, 27783 dfs, $\nu = 0.3$ , for $E$ see the text							
$E_1/E_2$	$n_s$	$\deg(M)$	Z	$N_{it}$	$T_{CPU}$	$\rho$	cond
1	27	4	27	4	45 + 19	0.06	1.26
10	27	4	27	4	45 + 19	0.06	1.26
100	27	4	27	5	45 + 23	0.08	1.37
1000	27	4	27	5	45 + 23	0.08	1.39
100000	27	4	27	4	45 + 19	0.08	1.29

*Local BC:* Zero boundary condition at all corners of the lower face and adjacent surface nodes.

*Point BC:*

$$\begin{aligned} u_1([0, 0, 0]) &= u_2([0, 0, 0]) = u_3([0, 0, 0]) = 0, \\ u_1([1, 0, 0]) &= u_2([1, 0, 0]) = 0, \\ u_3([1, 1, 0]) &= 0. \end{aligned}$$

Again, in accord with the theory, the convergence rate does not change even with variationally problematic conditions, i.e., when the Dirichlet boundary condition was specified on a set of zero measure.

*Randomly distributed Young modulus.* Our final set of experiments on the unit cube is concerned with Young moduli having randomly distributed values throughout the domain. The Poisson ratio was 0.3 in all the experiments. We use the following designations in Table 5.

*Random 100:* The Young moduli 0.1, 1, 10 have been assigned pseudo-randomly to elements.

*Random 1000:* The Young moduli 0.1, 1, 100 have been assigned pseudo-randomly to elements.

Uniform distribution of the three values of Young modulus has been used in both experiments. This distribution of jumps throughout the domain is not supported by

TABLE 4  
*Uniformity of convergence with respect to boundary conditions.*

9261 nodes, 27783 degrees of freedom, $E = \text{const}, \nu = 0.3$							
Experiment	$n_s$	$\text{deg}(M)$	Z	$N_{it}$	$T_{CPU}$	$\rho$	cond
Face BC	27	4	16	5	47 + 23	0.10	1.42
Face BC	343	1	23	5	33 + 20	0.09	1.37
Local BC	27	4	19	6	48 + 29	0.11	1.56
Local BC	343	1	24	6	31 + 22	0.10	1.48
Point BC	27	4	19	6	47 + 29	0.11	1.57
Point BC	343	1	24	6	32 + 22	0.10	1.46

TABLE 5  
*Experimental results for randomly distributed Young modulus.*

9261 nodes, 27783 degrees of freedom, $E = \text{random}, \nu = 0.3$							
Experiment	$n_s$	$\text{deg}(M)$	Z	$N_{it}$	$T_{CPU}$	$\rho$	cond
Random 100	27	4	20	9	49 + 45	0.26	2.88
Random 100	343	1	24	9	32 + 33	0.23	2.64
Random 1000	27	4	20	20	49 + 90	0.51	12.5
Random 1000	343	1	24	19	31 + 63	0.50	11.0

the theory, but the algorithm proves to be robust as can be seen from Table 5.

*Turbine.* Finally, in Table 6 we show the convergence results for a real-life problem. Several requirements of the theory were not met here. Thin elements on the blades violate the quasi-uniformity condition of the mesh, and the small thickness of the blades results in singularly perturbed behavior of the equation.

**7. Acknowledgement.** The authors would like to thank Professor Jinchao Xu for many useful comments on an earlier version of this paper.

#### REFERENCES

- [1] R. A. ADAMS, *Sobolev Spaces*, Academic press, New York, 1975.
- [2] O. AXELSSON AND I. GUSTAFFSON, *Iterative methods for the solution of the Navier equations of elasticity*, *Comput. Methods Appl. Mech. Engrg.*, 15 (1978), pp. 241–258.
- [3] C. BÖRGERS, *The Neumann–Dirichlet domain decomposition method with inexact solvers on the subdomains*, *Numer. Math.*, 55 (1989), pp. 123–136.
- [4] J. H. BRAMBLE, *Multigrid Methods*, Pitman Res. Notes Math. Sci. Ser., 294, Longman Scientific & Technical, Harlow, England, 1993.
- [5] J. H. BRAMBLE, J. E. PASCIAK, AND A. H. SCHATZ, *The construction of preconditioners for elliptic problems by substructuring, I*, *Math. Comp.*, 47 (1986), pp. 103–134.
- [6] J. H. BRAMBLE, J. E. PASCIAK, AND A. T. VASILLEV, *Analysis of non-overlapping domain decomposition algorithms with inexact solvers*. To appear, 1996.
- [7] J. H. BRAMBLE, J. E. PASCIAK, J. WANG, AND J. XU, *Convergence estimates for multigrid algorithms without regularity assumptions*, *Math. Comp.*, 57 (1991), pp. 23–45.
- [8] A. BRANDT, *Algebraic multigrid theory: The symmetric case*, *Appl. Math. Comput.*, 19 (1986), pp. 23–56.
- [9] S. C. BRENNER AND L. R. SCOTT, *The Mathematical Theory of Finite Element Methods*, Springer-Verlag, New York, 1994.
- [10] M. BREZINA, *Robust Iterative Solvers on Unstructured Meshes*, Ph.D. thesis, University of Colorado at Denver, Denver, CO, 1997.



TABLE 6

Results for turbine (Boundary conditions: Dirichlet, on a set of zero measure).

Turbine, 41040 nodes, 123120 degrees of freedom							
Experiment	$n_s$	$\deg(M)$	Z	$N_{it}$	$T_{CPU}$	$\rho$	cond
Turbine	1730	1	22	12	85 + 240	0.39	16.0

- [11] T. F. CHAN, S. MARGENOV, AND P. VASSILEVSKI, *Performance of block-ILU factorization preconditioners based on block-size reduction for 2D elasticity systems*, Tech. report 94-33, Department of Math., UCLA, Los Angeles, CA, 1994, CAM Report.
- [12] C. M. DAFERMOS, *Some remarks on Korn's inequality*, Z. Angew. Math. Phys., 19 (1968), pp. 913–920.
- [13] M. DRYJA, B. F. SMITH, AND O. B. WIDLUND, *Schwarz analysis of iterative substructuring algorithms for elliptic problems in three dimensions*, SIAM J. Numer. Anal., 31 (1994), pp. 1662–1694.
- [14] G. E. FORSYTHE AND E. G. STRAUSS, *On the best conditioned matrices*, Proc. Amer. Math. Soc., 6 (1955), pp. 340–345.
- [15] V. KONDRATIEV AND O. OLBINIK, *Hardy's and Korn's Type Inequalities and their Applications*, Rend. Mat. Appl. (7) 10 (1990), pp. 641–666.
- [16] J. KRÍŽKOVÁ AND P. VANĚK, *Two-level preconditioner with small coarse grid appropriate for unstructured meshes*, Numer. Linear Algebra Appl., 3 (1996), pp. 255–274.
- [17] J. MANDEL, *Balancing domain decomposition*, Comm. Numer. Methods Engrg., 9 (1993), pp. 233–241.
- [18] A. VAN DER SLUIS, *Condition number and equilibration of matrices*, Numer. Math., 14 (1969), pp. 14–23.
- [19] P. VANĚK, *Acceleration of convergence of a two-level algorithm by smoothing transfer operator*, Appl. Math., 37 (1992), pp. 265–274.
- [20] P. VANĚK AND J. KRÍŽKOVÁ, *Two-Level Method on Unstructured Meshes with Convergence Rate Independent of the Coarse-Space Size*, Tech. Report 35, Center for Computational Mathematics, University of Colorado at Denver, Denver, CO, 1995.
- [21] P. VANĚK, J. MANDEL, AND M. BREZINA, *Algebraic Multigrid on Unstructured Meshes*, UCD/CCM Report 34, Center for Computational Mathematics, University of Colorado at Denver, Denver, CO, 1994.
- [22] P. VANĚK, J. MANDEL, AND M. BREZINA, *Algebraic multigrid by smoothed aggregation for second and fourth order elliptic problems*, Computing, 56 (1996), pp. 179–196.
- [23] P. VANĚK, J. MANDEL, AND M. BREZINA, *Solving a Two-Dimensional Helmholtz Problem Using Algebraic Multigrid*, UCD/CCM Report 110, Center for Computational Mathematics, University of Colorado at Denver, Denver, CO, 1997.
- [24] P. VANĚK, R. TEZAUER, M. BREZINA, AND J. KRÍŽKOVÁ, *Two-level method with coarse space size independent convergence*, in Domain Decomposition Methods in Sciences and Engineering, R. Glowinski, J. Périaux, Z. Shi, and O. Widlund, eds., John Wiley & Sons, New York, 1997.